Crystal structure of rilpivirine, $C_{22}H_{18}N_6$

James A. Kaduk,[1,a] Kai Zhong,[2] and Thomas N. Blanton[2]
[1]*Illinois Institute of Technology, 3101 S. Dearborn St., Chicago, Illinois 60616*
[2]*ICDD, 12 Campus Blvd., Newtown Square, Pennsylvania 19073-3273*

(Received 12 September 2014; accepted 3 March 2015)

The crystal structure of rilpivirine has been solved and refined using synchrotron X-ray powder diffraction data, and optimized using density functional techniques. Rilpivirine crystallizes in space group $P2_1/c$ (#14) with a = 8.39049(3), b = 13.89687(4), c = 16.03960(6) Å, β = 90.9344(3)°, V = 1869.995(11) Å^3, and Z = 4. The most prominent features of the structure are N–H···N hydrogen bonds. These form a $R2,2(8)$ pattern which, along with $C1,1(12)$ and longer chains, yield a three-dimensional hydrogen bond network. The powder pattern has been submitted to International Centre for Diffraction Data, ICDD, for inclusion in future releases of the Powder Diffraction File™. © *2015 International Centre for Diffraction Data.*
[doi:10.1017/S0885715615000196]

Key words: rilpivirine, Edurant, powder diffraction, Rietveld, density functional theory

I. INTRODUCTION

Rilpivirine (TMC278, trade name Edurant) was developed by Tibotec for the treatment of acquired immunodeficiency syndrome (AIDS) caused by the human immunodeficiency virus (HIV) infection. Rilpivirine works as a second-generation non-nucleoside reverse transcriptase inhibitor (NNRTI) (Goebel *et al.*, 2006), and was approved by the U.S. Food and Drug Administration (USFDA) in May 2011. It has the systematic name 4-{[4-({4-[(*E*)-2-cyanovinyl]2,6-dimethylphenyl}amino)pyrimidin-2-yl]amino} benzonitrile. A two-dimensional molecular structural diagram is shown in Figure 1.

The presence of high-quality reference powder patterns in the Powder Diffraction File (PDF; ICDD, 2014) is important for phase identification, particularly by pharmaceutical, forensic, and law enforcement scientists. The crystal structures of a significant fraction of the largest dollar volume pharmaceuticals have not been published, and thus calculated powder patterns are not present in the PDF-4 databases. Sometimes experimental patterns are reported, but they are generally of low quality. Accordingly, a collaboration among ICDD, Illinois Institute of Technology (IIT), Poly Crystallography Inc., and Argonne National Laboratory has been established to measure high-quality synchrotron powder patterns of commercial pharmaceutical ingredients, to include these reference patterns in the PDF, and to determine the crystal structures of these Active Pharmaceutical Ingredients (APIs).

Even when the crystal structure of an API is reported, the single-crystal structure was often determined at low temperature. Most powder measurements are performed at ambient conditions. Thermal expansion (often anisotropic) means that the peak positions calculated from a low-temperature single-crystal structure often differ significantly from those measured at ambient conditions. These peak shifts can result in failure of default search/match algorithms to identify a phase, even when it is present in the sample. High-quality reference patterns measured at ambient conditions are thus critical for easy identification of APIs using standard powder diffraction practices.

II. EXPERIMENTAL

Rilpivirine was commercial reagent, purchased from Carbosynth Company (Lot #FR158451201F), and was used as-received. The white powder was packed into a 1.5 mm diameter Kapton capillary, and rotated during the experiment at ~50 cycles s^{-1}. The powder pattern was measured at 295 K at beam line 11-BM (Lee *et al.*, 2008; Wang *et al.*, 2008) of

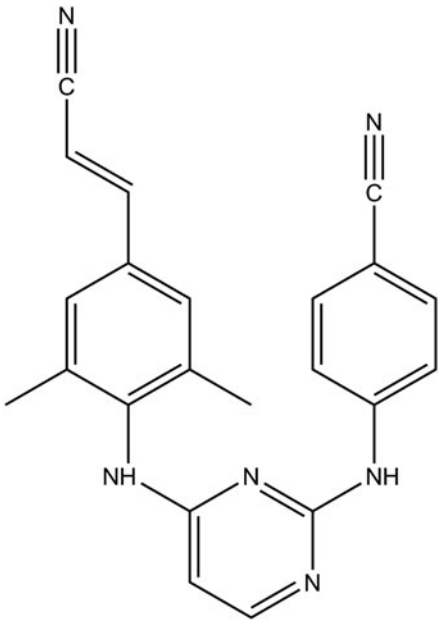

Figure 1. The molecular structure of rilpivirine.

[a]Author to whom correspondence should be addressed. Electronic mail: kaduk@polycrystallography.com

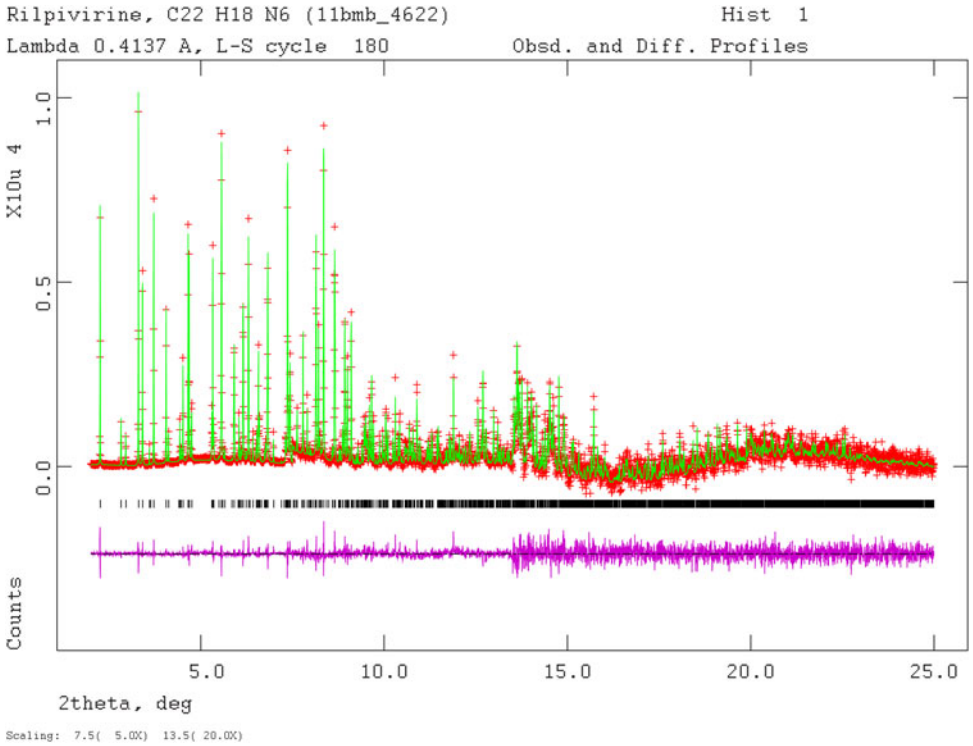

Figure 2. (Color online) The Rietveld plot for the refinement of rilpivirine. The red crosses represent the observed data points, and the green line is the calculated pattern. The magenta curve is the difference pattern, plotted at the same vertical scales as the other patterns. The vertical scale has been multiplied by a factor of 5 for $2\theta > 7.5°$, and by a factor of 20 for $2\theta > 13.5°$.

the Advanced Photon Source at Argonne National Laboratory using a wavelength of 0.413691 Å from 0.5° to 50° 2θ with a step size of 0.001° and a counting time of 0.1 s per step; the total exposure to the beam was ~1.3 h. The pattern was indexed on a primitive monoclinic unit cell having a = 8.390, b = 13.895, c = 16.039 Å, β = 90.9°, and V = 1869.6 Å^3 using Jade 9.5 (MDI, 2013). A search of this cell in the Cambridge Structural Database (CSD; Allen, 2002) yielded 104 hits, but no crystal structure for rilpivirine. The systematic absences determined the space group to be $P2_1/c$ (a common space group for organic compounds), which was confirmed by successful solution and refinement of the structure.

A rilpivirine molecule was built and its conformation optimized using Spartan '14 (Wavefunction, 2013), and saved as a mol2 file. This file was converted into a Fenske–Hall *Z*-matrix file using OpenBabel (O'Boyle *et al.*, 2011). This molecule was used to solve the structure with FOX (Favre-Nicolin and Černý, 2002). The maximum $\sin\theta/\lambda$ used in the solution was 0.3 Å^{-1}.

Rietveld refinement was carried out using GSAS (Larson and Von Dreele, 2004). Only the 2°–25° 2θ portion of the pattern was included in the refinement. The two phenyl groups were refined as rigid bodies. All non-H bond distances and angles were subjected to restraints, based on a Mercury/Mogul Geometry Check (Bruno *et al.*, 2004; Sykes *et al.*, 2011) of the molecule. The Mogul average and standard deviation for each quantity were used as the restraint parameters. The N1–C6 aromatic ring was subjected to a planar restraint with a standard deviation of 0.01 Å. The restraints contributed 2.78% to the final χ^2. Isotropic displacement coefficients were refined, grouped by chemical similarity. The hydrogen atoms were included in calculated positions, which were recalculated during the refinement. The U_{iso} of each hydrogen atom was constrained to be 1.3× that of the heavy atom to which it is attached. The peak profiles were described using profile function #4, which includes the Stephens (1999) anisotropic strain-broadening model. The background was modeled using a three-term shifted Chebyshev polynomial and a ten-term diffuse scattering function to describe the scattering from the Kapton capillary and any amorphous content of the sample. The final refinement of 90 variables using 23 002 observations yielded the residuals wRp = 0.0699, Rp = 0.0568, DWd = 0.828, and χ^2 = 1.307. The largest peak (1.26 Å from C18) and hole (0.63 Å from C15) in the difference Fourier map were 0.21 and −0.21 eÅ^{-3}, respectively. The Rietveld plot is included as Figure 2. The largest errors are in the shapes of the lowest-angle peaks, and may reflect subtle changes in the specimen during the measurement.

A density functional geometry optimization (fixed experimental unit cell) was carried out using CRYSTAL09 (Dovesi *et al.*, 2005). The basis sets for the H, C, and N atoms were those of Gatti *et al.* (1994). The calculation used eight *k*-points and the B3LYP functional.

III. RESULTS AND DISCUSSION

The refined atom coordinates of rilpivirine are reported in Table I, and the coordinates from the density functional theory (DFT) optimization in Table II. The root-mean-square deviation of the non-hydrogen atoms is 0.09 Å, and the maximum deviation is 0.16 Å, at C14 (Figure 3). The discussion of the geometry uses the DFT-optimized structure. The asymmetric unit (with atom numbering) is illustrated in Figure 4, and

https://doi.org/10.1017/S0885715615000196 Published online by Cambridge University Press

TABLE I. Rietveld refined fractional coordinates of rilpivirine. Space group $P2_1/c$, a = 8.39049(3) Å, b = 13.89687(4) Å, c = 16.03960(6) Å, β = 90.9344(3)°, V = 1869.995(11) Å^3, and Z = 4.

Name	X	Y	Z	U_i, Å^2
N1	0.72746(26)	0.69610(15)	0.10622(16)	0.0465(7)
C2	0.64709(27)	0.62892(13)	0.06149(11)	0.0465(7)
N3	0.50478(28)	0.59072(10)	0.07921(15)	0.0465(7)
C4	0.43889(21)	0.62424(16)	0.14902(18)	0.0465(7)
C5	0.50889(31)	0.69258(16)	0.19986(13)	0.0465(7)
C6	0.65642(28)	0.72729(11)	0.17552(14)	0.0465(7)
N7	0.72777(34)	0.80208(19)	0.21809(14)	0.0465(7)
C8	0.85772(22)	0.85508(14)	0.18841(15)	0.0431(6)
C9	1.00864(25)	0.81364(15)	0.18634(16)	0.0431(6)
C10	1.13576(23)	0.86495(21)	0.15375(18)	0.0431(6)
C11	1.11197(28)	0.95770(20)	0.12323(17)	0.0431(6)
C12	0.96105(32)	0.99914(14)	0.12530(17)	0.0431(6)
C13	0.83392(24)	0.94783(14)	0.15789(17)	0.0431(6)
C14	1.04091(44)	0.71737(24)	0.22686(29)	0.0601(8)
C15	0.67039(37)	0.99206(25)	0.15691(29)	0.0601(8)
C16	1.25111(47)	1.00838(31)	0.08934(35)	0.0601(8)
C17	1.25707(50)	1.09835(32)	0.07360(36)	0.0601(8)
C18	1.40276(56)	1.14349(25)	0.04259(34)	0.0601(8)
N19	1.51850(45)	1.17250(27)	0.01581(27)	0.0601(8)
N20	0.71664(34)	0.59366(25)	−0.00837(19)	0.0465(7)
C21	0.86934(27)	0.60717(21)	−0.04135(17)	0.0431(6)
C22	0.97716(35)	0.67405(18)	−0.00890(15)	0.0431(6)
C23	1.13047(31)	0.67961(18)	−0.04044(18)	0.0431(6)
C24	1.17596(26)	0.61829(21)	−0.10441(19)	0.0431(6)
C25	1.06814(34)	0.55142(17)	−0.13686(14)	0.0431(6)
C26	0.91483(30)	0.54586(18)	−0.10533(16)	0.0431(6)
C27	1.33324(39)	0.62130(40)	−0.13856(27)	0.0601(8)
N28	1.45422(39)	0.62103(33)	−0.16917(24)	0.0601(8)
H29	0.313480	0.598140	0.173630	0.0605(9)
H30	0.442530	0.720220	0.262360	0.0605(9)
H31	0.685560	0.825730	0.282450	0.0605(9)
H32	1.258460	0.827470	0.152480	0.0560(8)
H33	0.945340	1.074260	0.102650	0.0560(8)
H34	1.037100	0.655730	0.175460	0.0782(10)
H35	0.943790	0.696970	0.273720	0.0782(10)
H36	1.161500	0.713740	0.258440	0.0782(10)
H37	0.577140	0.935280	0.172800	0.0782(10)
H38	0.643320	1.017280	0.088360	0.0782(10)
H39	0.662900	1.055170	0.199380	0.0782(10)
H40	1.370710	0.966040	0.083080	0.0782(10)
H41	1.135720	1.140100	0.081180	0.0782(10)
H42	0.639830	0.550110	−0.051210	0.0605(9)
H43	0.936940	0.722880	0.045820	0.0560(8)
H44	1.214490	0.733950	−0.013000	0.0560(8)
H45	1.099000	0.501580	−0.188850	0.0560(8)
H46	0.821440	0.490490	−0.130010	0.0560(8)

TABLE II. DFT (CRYSTAL09) optimized fractional coordinates of rilpivirine. Space group $P2_1/c$, a = 8.39049(3) Å, b = 13.89687(4) Å, c = 16.03960(6) Å, β = 90.9344(3)°, V = 1869.995(11) Å^3, and Z = 4.

Name	X	Y	Z	U_{iso} (Å^2)
N1	0.71980	0.69920	0.10293	0.04650
C2	0.64411	0.62871	0.06160	0.04650
N3	0.50319	0.58882	0.08134	0.04650
C4	0.44084	0.62231	0.15211	0.04650
C5	0.50909	0.69263	0.20162	0.04650
C6	0.65188	0.73284	0.17210	0.04650
N7	0.72296	0.80773	0.21382	0.04650
C8	0.85681	0.85934	0.18420	0.04310
C9	1.00762	0.81531	0.18240	0.04310
C10	1.13459	0.86728	0.14965	0.04310
C13	0.83576	0.95569	0.15842	0.04310
C14	1.03288	0.71519	0.21583	0.06010
C15	0.67284	1.00095	0.15684	0.06010
C16	1.25585	1.01179	0.08982	0.06010
C17	1.27312	1.10707	0.07516	0.06010
C18	1.41700	1.14348	0.04171	0.06010
N19	1.53625	1.17166	0.01443	0.06010
N20	0.71352	0.59049	−0.00853	0.06010
C21	0.86405	0.60605	−0.04087	0.04310
C22	0.97171	0.67883	−0.01470	0.04310
C23	1.12310	0.68462	−0.04843	0.04310
C24	1.17113	0.61973	−0.11038	0.04310
C25	1.06280	0.54930	−0.13883	0.04310
C26	0.91312	0.54300	−0.10452	0.04310
C27	1.32708	0.62410	−0.14426	0.06010
N28	1.45360	0.62626	−0.17296	0.06010
C12	0.96633	1.00650	0.12900	0.04310
C11	1.11680	0.96297	0.12296	0.04310
H29	0.32937	0.59023	0.17112	0.06050
H30	0.45607	0.71782	0.25859	0.06050
H31	0.65262	0.84048	0.25644	0.06050
H32	1.25092	0.83320	0.14660	0.06050
H33	0.94849	1.07979	0.10731	0.06050
H34	1.00579	0.66156	0.16774	0.07820
H35	0.95347	0.70124	0.26776	0.07820
H36	1.15608	0.70530	0.23710	0.07820
H37	0.60504	0.98773	0.21326	0.07820
H38	0.60301	0.97090	0.10489	0.07820
H39	0.68071	1.07843	0.14700	0.07820
H40	1.35440	0.96417	0.07554	0.07820
H41	1.18116	1.15982	0.08792	0.07820
H42	0.64762	0.53568	−0.03397	0.06050
H43	0.93765	0.72902	0.03312	0.05600
H44	1.20642	0.73926	−0.02666	0.05600
H45	1.09648	0.49927	−0.18732	0.05600
H46	0.83296	0.48642	−0.12481	0.05600

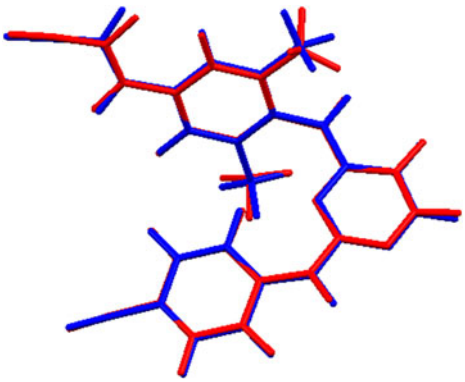

Figure 3. (Color online) Comparison of the refined and optimized structures of rilpivirine. The Rietveld refined structure is colored red and the DFT-optimized structure is in blue.

the crystal structure is presented in Figure 5. A stereo view of the structure is included as Supplemental Figure S1.

All bond distances and angles fall within the normal ranges indicated by a Mercury Geometry Check (Macrae *et al.*, 2008). Only the C16–C17–C18–N19 torsion angle of 6.9° (Z-score = 6.9) is flagged as unusual, but there are only three examples of this torsion angle in the CSD, so the score is not particularly meaningful. The Hirshfeld surface (Spackman and Jayatilaka, 2009) indicates that most of the intermolecular contacts are at or longer than the sums of the van der Waals radii (Figure 6). The only contacts shorter than the sums of the van der Waals radii are the hydrogen bonds. The volume enclosed by the Hirshfeld surface is 459.50 Å^3, which is smaller than one-fourth of the cell volume (467.50 Å^3). The molecules are relatively loosely packed. The small difference

https://doi.org/10.1017/S0885715615000196 Published online by Cambridge University Press

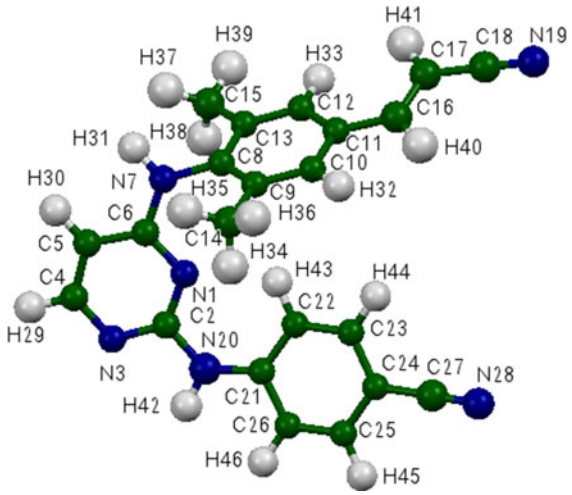

Figure 4. (Color online) The molecular structure of rilpivirine, with the atom numbering. The atoms are represented by 50% probability spheroids.

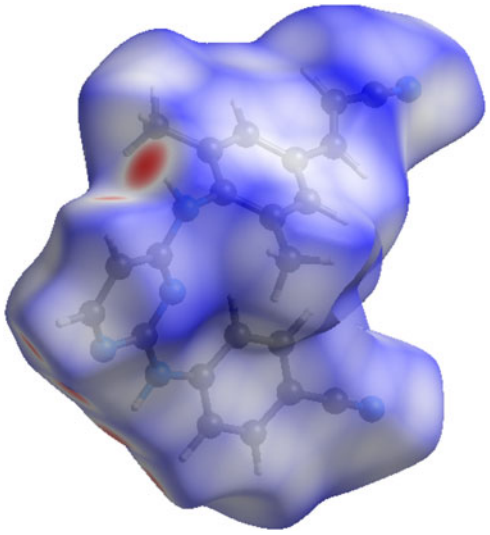

Figure 6. (Color online) The Hirshfeld surface of rilpivirine. Intermolecular contacts longer than the sums of van der Waals radii are colored blue, and contacts shorter than the sum of the radii are colored red. Contacts equal to the sum of the radii are white.

between the two volumes is consistent with the lack of voids in the crystal structure.

An analysis of the contributions to the total crystal energy using the Forcite module of Materials Studio (Accelrys, 2013) suggests that the bond and angle distortion terms are small, and that torsion angle contributions are moderate. The energy appears to be dominated by electrostatic contributions, which in this force-field-based analysis include hydrogen bonds. The hydrogen bonds are better analyzed using the results of the DFT calculation.

The most prominent features of the crystal structure are the N7–H31···N28 and N20–H42···N3 hydrogen bonds (Table III). These form a *R*2,2(8) pattern (Etter, 1990; Bernstein *et al.*, 1995; Shields, *et al.*, 2000) which, along with *C*1,1(12) and longer chains, result in a three-dimensional hydrogen bond network. The *C*1,1(12) chains run approximately along the [201] direction. Intra- and intermolecular C–H···N hydrogen bonds also contribute to the crystal energy.

The Bravais–Friedel–Donnay–Harker (Bravais, 1866; Friedel, 1907; Donnay and Harker, 1937) morphology suggests that we might expect blocky morphology for rilpivirine; no preferred orientation correction was necessary. The powder pattern of rilpivirine has been submitted to ICDD for inclusion in future releases of the PDF.

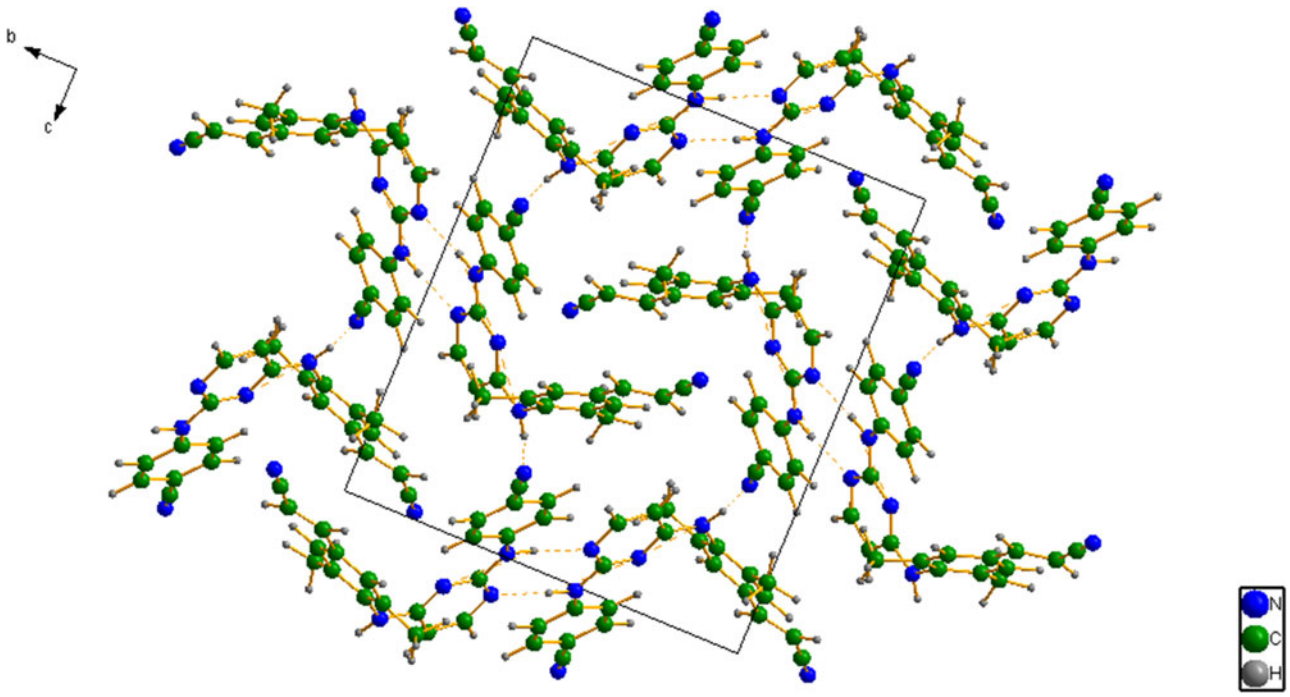

Figure 5. (Color online) The crystal structure of rilpivirine, viewed down the *a*-axis. The hydrogen bonds are shown as dashed lines.

https://doi.org/10.1017/S0885715615000196 Published online by Cambridge University Press

TABLE III. Hydrogen bonds in the DFT-optimized structure of rilpivirine.

D–H···*A*	*D*–H, (Å)	H···*A* (Å)	*D*···*A* (Å)	*D*–H···*A* (Å)	Overlap (*e*)
N7–H31···N28	1.018	2.085	3.063	160.4	0.044
N20–H42···N3	1.022	2.267	3.288	176.0	0.045
C14–H35···N7	1.092	2.574	2.901	96.1	0.010
C22–H43···N1	1.079	2.198	2.870	118.2	0.018
C5–H30···N28	1.081	2.429	3.260	132.6	0.012
C16–H40···N19	1.086	2.556	3.526	148.3	0.013
C23–H44···N19	1.086	2.494	3.522	157.6	0.021

ACKNOWLEDGMENTS

Use of the Advanced Photon Source at Argonne National Laboratory was supported by the U. S. Department of Energy, Office of Science, Office of Basic Energy Sciences, under Contract No. DE-AC02-06CH11357. This work was partially supported by the International Centre for Diffraction Data. We thank Lynn Ribaud for his assistance in data collection.

SUPPLEMENTARY MATERIALS AND METHODS

The supplementary material for this article can be found at http://www.journals.cambridge.org/PDJ

Accelrys (**2013**). *Materials Studio* 7.0 (Accelrys Software Inc., San Diego, CA).

Allen, F. H. (**2002**). "The Cambridge Structural Database: a quarter of a million crystal structures and rising," Acta Crystallogr. B, Struct. Sci. **58**, 380–388.

Bernstein, J., Davis, R. E., Shimoni, L., and Chang, N. L. (**1995**). "Patterns in hydrogen bonding: functionality and graph set analysis in crystals," Angew. Chem. Int. Ed. Engl., **34**(15), 1555–1573.

Bravais, A. (**1866**). *Etudes Cristallographiques* (Gauthier Villars, Paris).

Bruno, I. J., Cole, J. C., Kessler, M., Luo, J., Motherwell, W. D. S., Purkis, L. H., Smith, B. R., Taylor, R., Cooper, R. I., Harris, S. E., and Orpen, A. G. (**2004**). "Retrieval of crystallographically-derived molecular geometry information," J. Chem. Inf. Sci. **44**, 2133–2144.

Donnay, J. D. H. and Harker, D. (**1937**). "A new law of crystal morphology extending the law of Bravais," Am. Mineral. **22**, 446–467.

Dovesi, R., Orlando, R., Civalleri, B., Roetti, C., Saunders, V. R., and Zicovich-Wilson, C. M. (**2005**). "CRYSTAL: a computational tool for the *ab initio* study of the electronic properties of crystals," Z. Kristallogr. **220**, 571–573.

Etter, M. C. (**1990**). "Encoding and decoding hydrogen-bond patterns of organic compounds," Acc. Chem. Res. **23**(4), 120–126.

Favre-Nicolin, V. and Černý, R. (**2002**). FOX, "Free Objects for crystallography: a modular approach to ab initio structure determination from powder diffraction," J. Appl. Crystallogr. **35**, 734–743.

Friedel, G. (**1907**). "Etudes sur la loi de Bravais," Bull. Soc. Fr. Mineral. **30**, 326–455.

Gatti, C., Saunders, V. R., and Roetti, C. (**1994**). "Crystal-field effects on the topological properties of the electron-density in molecular crystals - the case of urea," J. Chem. Phys. **101**, 10686–10696.

Goebel, F., Yakovlev, A., Pozniak, A. L., Vinogradova, E., Boogaerts, G., Hoetelmans, R., de Béthune, M. P., Peeters, M., and Woodfall, B. (**2006**). "Short-term antiviral activity of TMC278 — a novel NNRTI — in treatment-naive HIV-1-infected subjects," AIDS **20**(13), 1721–1726.

ICDD (**2014**), PDF-4+ 2014 (Database). *International Centre for Diffraction Data*, edited by Dr. Soorya Kabekkodu (Newtown Square, PA, USA).

Larson, A. C. and Von Dreele, R. B. (**2004**). "General Structure Analysis System, (GSAS)", Los Alamos National Laboratory Report LAUR 86–784.

Lee, P. L., Shu, D., Ramanathan, M., Preissner, C., Wang, J., Beno, M. A., Von Dreele, R. B., Ribaud, L., Kurtz, C., Antao, S. M., Jiao, X., and Toby, B. H. (**2008**). "A twelve-analyzer detector system for high-resolution powder diffraction," J. Synch. Radiat. **15**(5), 427–432.

Macrae, C. F., Bruno, I. J., Chisholm, J. A., Edington, P. R., McCabe, P., Pidcock, E., Rodriguez-Monge, L., Taylor, R., van de Streek, J., and Wood, P. A. (**2008**). "Mercury CSD 2.0 – new features for the visualization and investigation of crystal structures," J. Appl. Crystallogr. **41**, 466–470.

MDI (**2013**). *Jade 9.5* (Materials Data. Inc., Livermore, CA).

O'Boyle, N., Banck, M., James, C. A., Morley, C., Vandermeersch, , and Hutchison, G. R. (**2011**). "Open Babel: an open chemical toolbox," J. Chem. Inf. **3**, 33.

Shields, G. P., Raithby, P. R., Allen, F. H., and Motherwell, W. S. (**2000**). "The assignment and validation of metal oxidation states in the Cambridge Structural Database," Acta Crystallogr. B, Struct. Sci. **56**(3), 455–465.

Spackman, M. A. and Jayatilaka, D. (**2009**). "Hirshfeld surface analysis," Cryst. Eng. Commun. **11**, 19–32.

Stephens, P. W. (**1999**). "Phenomenological model of anisotropic peak broadening in powder diffraction," J. Appl. Crystallogr. **32**, 281–289.

Sykes, R. A., McCabe, P., Allen, F. H., Battle, G. M., Bruno, I. J., and Wood, P. A. (**2011**). "New software for statistical analysis of Cambridge Structural Database data," J. Appl. Crystallogr. **44**, 882–886.

Wang, J., Toby, B. H., Lee, P. L., Ribaud, L., Antao, S. M., Kurtz, C., Ramanathan, M., Von Dreele, R. B., and Beno, M. A. (**2008**). "A dedicated powder diffraction beamline at the Advanced Photon Source: commissioning and early operational results," Rev. Sci. Instrum. **79**, 085105.

Wavefunction, Inc. (**2013**). Spartan '14 Version 1.1.0, Wavefunction Inc., 18401 Von Karman Ave., Suite 370, Irvine CA 92612.